Potential Conflict Identification of Terminal-Area Traffic Flow Based on Three-Dimensional Trajectory Tube Structures

LI Nan[1*], *LIU Xinrui*[1], *PENG Jiayi*[2], *ZHU Yan*[3], *WANG Hongyong*[1]

1. College of Air Traffic Management, Civil Aviation University of China, Tianjin 300300, P. R. China;
2. Airspace Management Center, Civil Aviation Administration of China Air Traffic Management Bureau, Beijing 101300, P. R. China; 3. Civil Aviation Administration of China Xinjiang Air Traffic Management Bureau, Urumqi 519015, P. R. China

(Received 21 March 2026; revised 9 April 2026; accepted 17 July 2026)

Abstract: With the rapid development of aviation industry, the density of terminal-airspace traffic has increased significantly, resulting in higher potential conflict among aircraft. To address this issue, this study proposes a potential conflict identification method for terminal airspace based on three-dimensional (3D) trajectory tube structures. The approach first clusters arrival trajectories to identify major traffic flows and constructs corresponding 3D trajectory tubes. It then introduces traffic-flow parameters into a probabilistic model, which is combined with three-dimensional airspace gridding to identify and locate potential conflict regions. The results demonstrate that the proposed method can effectively detect potential conflict areas within a 15 min time window and analyze the interactions among traffic flows within these regions. This research provides a valuable framework for improving the safety and efficiency of terminal airspace operations, offering both theoretical and practical significance for airspace optimization and decision-support enhancement.

Key words: terminal area; traffic flow; potential conflict identification; kernel density estimation; trajectory tube

CLC number: V355 **Document code:** A **Article ID:** 1005-1120(2026)04-0614-17

0 Introduction

As the critical hub of air traffic operations, the terminal airspace faces core challenges in managing the dynamic characteristics of traffic flow and ensuring operational safety, both of which are essential for improving the efficiency of airport cluster systems and the performance of air traffic management. As air transport demand continues to grow, terminal airspace has become increasingly congested, characterized by frequent trajectory intersections and convergences. This has intensified potential conflict risks and created an urgent need for precise and efficient conflict detection and early-warning technologies. Against this backdrop, an in-depth investigation into the structure of terminal air traffic flows and the underlying mechanisms of conflict is of great theoretical and practical significance for achieving system-level airspace optimization and enhancing decision-support capabilities in air traffic control.

Conflict detection is classified into short-term, medium-term, and long-term types, depending on the time scale and application purpose. Short-term conflict detection (typically within 5 min) focuses on real-time alerting and resolution, primarily relying on traffic alert and collision avoidance system (TCAS) or high-precision trajectory prediction algorithms to mitigate immediate collision risks. Medium-term conflict detection (typically for 10—20 min) serves as the bridge between tactical warning and strategic management. Its core lies in supporting controllers, flow coordination and collaborative decision-making through traffic flow modeling

*Corresponding author, E-mail address: nanli@cauc.edu.cn.

How to cite this article: LI Nan, LIU Xinrui, PENG Jiayi, et al. Potential conflict identification of terminal-area traffic flow based on three-dimensional trajectory tube structures[J]. Transactions of Nanjing University of Aeronautics and Astronautics, 2026, 43(4): 614-630.

http://dx.doi.org/10.16356/j.1005-1120.2026.04.009

and airspace complexity assessment. Long-term conflict detection (beyond 30 min) belongs to the strategic level and focuses on sector workload estimation, traffic demand forecasting, and flight slot allocation.

Conflict detection has long been a key research topic in air traffic management, and a variety of methodological approaches have been developed over the years. Early studies primarily relied on deterministic separation criteria, such as protection-zone models, minimum-separation thresholds, and rule-based systems, to identify short-term aircraft-to-aircraft conflicts for immediate alerting and resolution[1-4]. With the advancement of data-driven techniques, some works have incorporated deep learning and reinforcement learning frameworks to enhance short-horizon trajectory prediction, thereby improving tactical conflict alerting performance[5-6]. These methods have significantly contributed to improving the accuracy of short-term conflict detection.

At broader temporal scales, several studies have examined conflict characteristics from structural and complexity-based perspectives. Representative research includes analyzing the conflict risks of weaving routes using trajectory-tube structures, identifying critical conflict-prone grid regions through complex-network methods, and evaluating terminal-area operational orderliness through dynamic-density and distributed three-dimensional (3D) complexity[7-12]. Complex-network-based analyses have also been used to assess sector-level safety performance and identify potential conflict nodes at the network level[13]. In addition, the influence of intersecting route structures on potential conflicts has attracted attention, with studies investigating how route geometry, speed differentials, and sequencing patterns affect conflict occurrence near route intersections[14]. These works reveal conflict formation mechanisms from different viewpoints and provide important foundations for understanding instability in terminal-area operations.

In addressing operational uncertainty, researchers have increasingly shifted from deterministic judgment toward probabilistic risk modeling. Monte Carlo simulation, extreme-value theory, stochastic differential equations, and Bayesian spatiotemporal prediction have been widely used to characterize trajectory uncertainty and estimate conflict probabilities[15-18]. Some studies have further integrated conflict probability into trajectory-planning frameworks to support strategic, risk-aware decision-making[19]. To provide spatial representations of conflict risk, grid-based airspace discretization methods have also been proposed, transforming continuous airspace into computationally tractable grid structures that facilitate regional conflict-risk analysis and hotspot identification[20-22]. These methods demonstrate the value of combining probabilistic modeling with spatial discretization for refined conflict-risk assessment.

Recent studies on conflict detection have shown a clear shift from deterministic judgment toward probabilistic assessment, and from continuous spatial analysis toward discretized grid-based processing. Probabilistic approaches, such as Monte Carlo simulation and extreme value theory, enhance the robustness of conflict detection by quantifying risks under uncertainty. Meanwhile, airspace gridding methods transform the complex continuous airspace into computationally manageable spatial units, providing a unified framework for both macroscopic complexity evaluation and microscopic conflict localization.

However, existing studies still exhibit certain limitations. Most works either focus on short-term, microscopic aircraft-to-aircraft conflict detection or on long-term, macroscopic airspace complexity measurement. Research that effectively couples the dynamic characteristics of traffic flows with probabilistic grid-based models, concentrates on the medium-term tactical warning level, and is capable of analyzing the causes of conflicts, namely flow-to-flow interactions, remains relatively scarce.

For clarity, the two key terms are defined as follows. “Causes of conflict” refer to the specific traffic flows whose mutual interactions engender conflict risks within potential conflict zones in the terminal area. “Flow-to-flow interactions” denote the mechanism by which different traffic flows influence one another as they intersect, converge, or approach each other in space. These interactions constitute the fundamental cause of conflict risk formation.

Therefore, this study proposes a data-driven 3D traffic flow generation method based on terminal-area automatic dependent surveillance-broadcast (ADS-B) arrival trajectory data. Building upon this framework, a probabilistic model is integrated to achieve the identification and characterization of potential conflict regions within the 3D terminal airspace. The proposed method can effectively detect potential conflict risk areas among different traffic flows within each 15 min time window. The overall process is as follows. First, terminal-area arrival trajectories are clustered to identify traffic flows and construct their corresponding 3D trajectory tubes. Second, traffic flow parameters are analyzed and characterized using kernel density estimation (KDE). Third, these parameters are incorporated into the potential conflict identification model. Finally, potential conflict hotspot regions within the gridded terminal airspace are identified. The study deepens the understanding of terminal air traffic flow structures and also provides valuable decision support for flow management, controller decision-making, and airspace design and analysis in complex terminal environments.

1 Construction of 3D Trajectory Tube Structure

1.1 Data preprocessing and normalization

In this study, ADS-B operational data from the terminal area of Beijing Daxing International Airport are used as the case dataset. The data cover a seven-day period from March 25 to March 31, 2024. After removing abnormal trajectory points and applying normalization and resampling procedures, a total of 2 485 valid arrival trajectories are obtained for subsequent analysis.

The raw data are preprocessed through the following procedures.

(1) Spatial and altitude filtering: Based on the terminal area boundary and altitude range (300—6 000 m), flight data corresponding to the approach phase is extracted, while data from ground operations and the final approach segment is excluded.

(2) Outlier removal: Under the assumption of flight continuity, any trajectory point pair with an altitude difference greater than 100 m between consecutive samples is considered abnormal and removed.

(3) Data smoothing: A moving average filter is applied to the latitude, longitude, and altitude coordinates to suppress signal noise and random fluctuations.

(4) Trajectory resampling: To ensure consistency for subsequent clustering analysis, each trajectory is resampled to generate a standardized sequence consisting of 50 evenly distributed points.

(5) Coordinate projection and normalization: The latitude and longitude data are transformed into a planar Cartesian coordinate system (x, y) centered on the airport using the Lambert conformal conic (LCC) projection. The projected coordinates are then normalized to eliminate dimensional effects and ensure consistency across different spatial scales.

1.2 Construction of 3D trajectory tube model

In this study, the density-based spatial clustering of applications with noise (DBSCAN) algorithm is employed to cluster arrival flight trajectories. The effectiveness of this algorithm has been validated from multiple perspectives and is well suited to the clustering analysis of terminal-area arrival trajectories. The key parameters of the algorithm are set as a neighborhood radius of $\varepsilon=0.060\ 0$ and a minimum number of core points of MinPts$=6$. These parameters are determined through multiple iterative experiments and optimization, enabling the algorithm to accurately capture the spatial distribution characteristics of arrival trajectories in the terminal area while effectively avoiding both over-clustering and under-clustering problems.

To quantitatively evaluate the clustering performance, the silhouette coefficient is adopted as the evaluation metric. The resulting silhouette coefficient reached 0.833 5, which falls within the excellent range of 0.7—1.0, indicating strong intra-cluster compactness and high inter-cluster separability.

In addition, as a density-based clustering method, DBSCAN does not require the number of clusters to be specified in advance. It can effectively identify and remove noise points in trajectory data, thereby reducing the influence of abnormal trajectories on the overall traffic flow pattern. Moreover, DBSCAN can adapt well to the non-uniform density distribution characteristics of terminal-area arrival trajectories. Compared with algorithms, like K-means, which require a predefined number of clusters, and hierarchical clustering methods that are sensitive to noise, DBSCAN is more suitable for clustering terminal-area arrival trajectories.

The clustering results obtained by the DBSCAN algorithm are highly consistent with the actual approach route layout of the studied terminal area. Therefore, they can realistically reflect the spatial structure of arrival traffic flows in the terminal area and provide reliable foundational data for the subsequent construction of 3D trajectory tube structures.

Given that some traffic flows in terminal airspace may extend over tens of kilometers, the altitude dimension is incorporated into the two-dimensional trajectory clustering results. The concepts of trajectory tube and trajectory tube window are introduced to construct a 3D traffic flow model. Each cluster corresponds to one trajectory tube, which contains an equal number of trajectory tube windows. The orientation of each window follows the flow direction of the clustered central trajectory, while the window size is determined by the extreme projection distances of all trajectory points along each spatial dimension. Fig.1 illustrates the clustering results of the arrival trajectories.

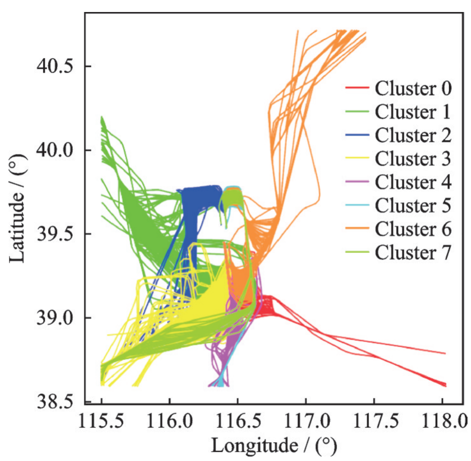

Fig.1 Arrival trajectory clustering results

The generation process of the trajectory tube is as follows.

(1) All trajectory points are grouped according to the clustering results, where each cluster corresponds to one trajectory tube.

(2) For each cluster, trajectory points are divided into multiple sequential windows based on time, with each window containing a fixed number of trajectory points.

(3) For each window, the centroid of all trajectory points within the window is calculated to represent its central position.

(4) For each window, a local coordinate system is constructed. The c axis is aligned with the global vertical direction. The b axis follows the direction of the central trajectory, pointing toward the centroid of the next window, representing the longitudinal direction of the trajectory. The a axis is orthogonal to both the b and c axes, representing the lateral direction of the trajectory.

(5) The width and the height of each window are determined by calculating the extreme projection distances of all trajectory points within the window along the lateral (a axis) and vertical (c axis) directions, respectively. Based on the centroid, the width, and the height, the boundary points of each trajectory tube window are generated.

(6) Each bounding box is defined as the convex hull formed between two consecutive windows within the same traffic flow.

(7) By connecting the bounding boxes of consecutive windows in each cluster, the complete trajectory tube corresponding to that traffic flow is constructed.

Fig. 2 illustrates the generation process of the trajectory tube. For each window, all trajectory points are orthogonally projected onto the local coordinate axes corresponding to the lateral and vertical directions of the window. Statistical analysis is then performed on the projected values to obtain the probability density functions (PDFs) of the lateral and vertical projections, referred to as the lateral and vertical PDFs, respectively. Fig.3 shows the trajectory tube and its structural representation.

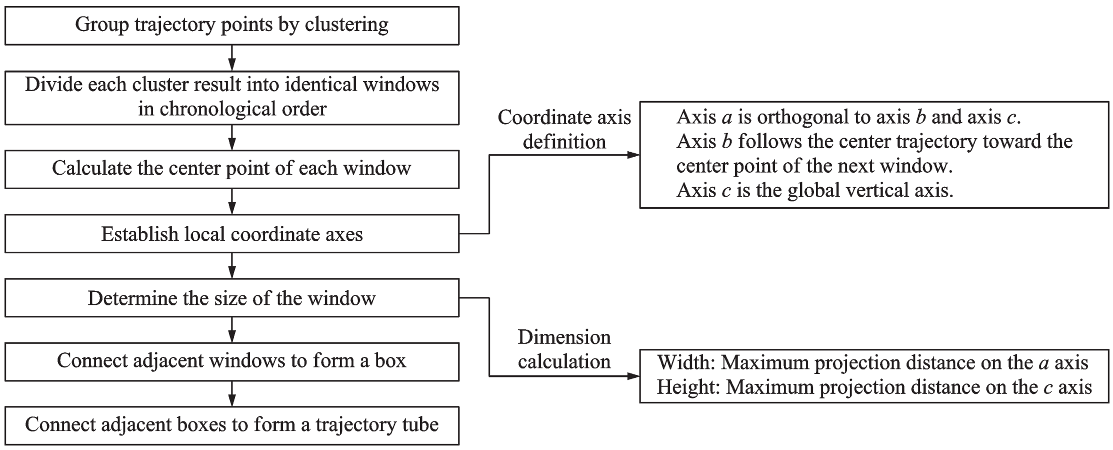

Fig.2 Trajectory tube generation steps

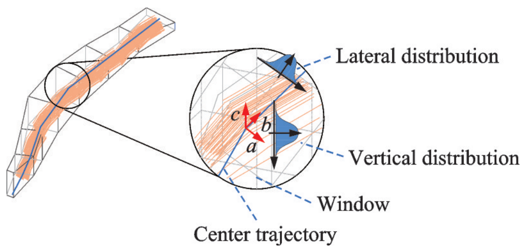

Fig.3 Trajectory tube and its structure

Based on the DBSCAN clustering results, a 3D trajectory tube structure is constructed in this study to achieve a structured 3D representation of arrival traffic flows in the terminal area. This approach overcomes the limitations of traditional two-dimensional trajectory analysis and microscopic single-aircraft analysis. The structural advantages and analytical value of the proposed trajectory tube model are reflected in two aspects.

First, by leveraging the clustering results, the collective characteristics of traffic flows can be effectively captured. Discrete individual arrival trajectories are integrated into flow structures with clearly defined spatial boundaries, enabling an intuitive representation of the spatial distribution patterns and interaction relationships among different traffic flows. This provides a foundation for flow-to-flow level analysis.

Second, a local coordinate system is established for each trajectory tube, consisting of three orthogonal directions: The longitudinal direction is aligned with the extended central flight trajectory; the vertical direction conforms to the global vertical axis; and the lateral direction is perpendicular to both the longitudinal and vertical axes. This coordinate system ensures that the spatial morphology of the trajectory tube is consistent with the actual motion trend of aircraft during the approach phase. As a result, the spatial distribution ranges and probability density characteristics of each traffic flow can be quantitatively described along the three directions. Statistical analysis further verifies that the lateral and vertical distributions are approximately independent, allowing joint analysis of traffic flow characteristics, such as speed distribution and arrival rate, together with the 3D spatial structure.

The proposed trajectory tube structure therefore provides a probabilistic analytical framework for medium- and short-term conflict identification at the flow-to-flow level. It enables a transition in conflict detection from microscopic individual-aircraft analysis to mesoscopic traffic-flow analysis, and from deterministic judgment to probabilistic assessment. Moreover, it establishes a solid structural and spatial foundation for the subsequent identification of conflict hotspots through 3D grid-based discretization of the terminal airspace.

In the trajectory tube generation model, it is assumed that the lateral and the vertical distributions are independent of each other. To validate this assumption, the correlation between the lateral and the vertical components of all trajectory tube windows is analyzed. The results show that the absolute values of 90% of the correlation coefficients are less than 0.16, indicating that most windows exhibit very weak correlations ($|r| < 0.3$ represents weak or no correlation). Therefore, it can be concluded that the lateral and the vertical distributions are statistically independent. Fig.4 presents the distribution of correlation coefficients between the lateral and the vertical components.

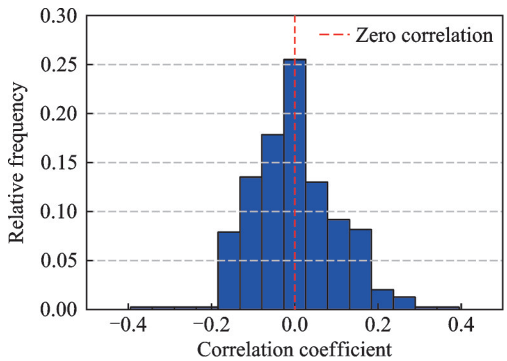

Fig.4 Distribution of lateral-vertical correlations

2 3D Traffic Flow Characteristics

To provide a more intuitive and accurate representation of 3D traffic flows, this study transforms the clustering results of flight trajectories into geometric representations by constructing trajectory tubes. This approach enables a clearer visualization of the dynamic characteristics of air traffic and the interactions among aircraft. The traffic flow characteristics considered in this study include speed distribution, arrival rate, and distance distribution, where the latter encompasses both inter-aircraft distance distribution and remaining distance distribution.

2.1 Speed distribution

During flight, aircraft speed exhibits variability influenced by multiple factors. Even within the same trajectory tube, flight speeds may differ due to various elements such as aircraft type, weather conditions, and air traffic control (ATC) instructions. In the terminal area in particular, controllers often adjust aircraft speeds to ensure flight safety, resulting in complex and dynamic patterns of speed distribution.

To accurately characterize the actual distribution of aircraft speed in the terminal area, this study applies the KDE method to analyze the speed data of each trajectory cluster. Unlike traditional approaches that rely on predefined distributional assumptions, KDE is a non-parametric density estimation technique. In this research, the Gaussian kernel function, widely used for modeling continuous variables, is adopted due to its ability to generate smooth probability density curves that align well with the continuous nature of speed data.

By constructing the speed distribution directly from empirical data without assuming any prior distribution, this method effectively captures complex or unknown statistical patterns, providing a more realistic representation of speed variations in terminal airspace operations. The Gaussian kernel density function is expressed as

$$f(x)=\frac{1}{nh}\sum_{i=1}^{n}K\left(\frac{v-v_i}{h}\right) \tag{1}$$

where n is the sample size of speed observations; h the smoothing bandwidth controlling kernel influence range; and $K(u)$ the Gaussian kernel function, and is expressed as

$$K(u)=\frac{1}{\sqrt{2\pi}}\mathrm{e}^{-\frac{1}{2}u^2} \tag{2}$$

The Gaussian kernel density distribution of the speed for each flow, including the extrema within the distribution, is stored for subsequent calculations.

2.2 Traffic flow arrival rate

Since this study focuses on the analysis of potential conflicts during aircraft arrivals in the terminal area, the time at which each aircraft reaches the terminal area boundary is defined as its arrival time. Since the number of aircraft within each clustering result (i. e., each traffic flow) varies, and some flows contain only a small number of aircraft, it is difficult to analyze the arrival process of each cluster individually. Therefore, the entire terminal airspace is treated as a single system for analysis, and the results are subsequently allocated to each traffic flow according to the proportional number of aircraft within that flow.

The arrival interval is calculated based on the difference in arrival times between successive aircraft. The entire day is divided into fixed 15 min time windows. According to probability theory, when the inter-arrival times of events are independent and identically distributed following an exponential distribution, the number of events occurring within a unit time follows a Poisson distribution. Hence, it is assumed that the aircraft arrival process within each time window is stationary and satisfies the exponential inter-arrival time distribution.

A unified analysis is conducted for all 15 min time windows throughout the day. The mean inter-arrival time t within each window is calculated using the method of moments to estimate the rate parameter λ of the exponential distribution

$$\lambda=\frac{1}{t} \tag{3}$$

The results show that in more than 80% of the 15 min time windows throughout the day, the chi-square test fails to reject the exponential distribution hypothesis, indicating that the arrival process during most time periods conforms to the exponential distribution property. During the period with the highest arrival rate, the exponential PDF is fitted, yielding a p-value of 0.475 5, which further verifies that the inter-arrival times follow an exponential distribution. This assumption forms the theoretical basis for the subsequent derivation of inter-aircraft distance distributions.

Meanwhile, the number of aircraft arrivals within each 15 min time window is calculated, and the mean number of arrivals per window is used to estimate the Poisson distribution parameter λ_j. The Poisson distribution is then fitted to the arrival count data within each time window. The results indicate that over 80% of the time windows pass the chi-square test for the Poisson distribution, demonstrating that the arrival process during most periods follows Poisson distribution characteristics. In the time window with the highest number of arrivals, the fitted p-value is 0.832 8, confirming that the arrival process during this period conforms to the Poisson distribution.

Since the number of aircraft arrivals within each cluster is relatively small in a 15 min interval, it is not feasible to establish an equivalent statistical model for each cluster individually. Therefore, it is assumed that all air routes are mutually independent and that their corresponding arrival processes are also independent. The overall aircraft arrival process in the terminal area is thus modeled as a non-homogeneous Poisson process, with the global arrival rate for each 15 min interval j denoted as Λ_j, defined as

$$\Lambda_j=\frac{N_j}{15\times 60} \tag{4}$$

where N_j denotes the total number of aircraft within the entire time interval j. The inter-arrival times follow an exponential distribution. For each trajectory tube i within the 15 min interval j, the arrival rate λ_i^j is derived by proportionally allocating the global arrival rate according to the traffic volume of each flow, as expressed by

$$\lambda_i^j=\pi_i^j\cdot\Lambda_j \tag{5}$$

where π_i^j represents the proportion of traffic volume for trajectory tube i within time interval j, defined as the ratio of the number of aircraft in trajectory tube i to the total number of aircraft across all trajectory tubes within the same interval j. Based on this, the arrival rate for each traffic flow in each time period is determined.

As the fact that the aircraft inter-arrival times within each 15 min interval follow an exponential distribution is verified and the arrival rate for each cluster is calculated, the average time interval of each trajectory tube is expressed as

$$\Delta t_i=\frac{1}{\lambda_i} \tag{6}$$

Its PDF is given by

$$f(\Delta t_i)=\lambda_i\cdot e^{\lambda_i\Delta t_i} \tag{7}$$

2.3 Distance distribution

2.3.1 Inter-aircraft distance distribution

The longitudinal distance between two consecutive aircraft is defined as the inter-aircraft distance, measured as the projection along the central trajectory. To capture the empirical characteristics of speed, the speed distribution is learned from data via KDE and combined with exponentially distributed inter-arrival times. Monte Carlo sampling is then used to generate inter-aircraft distance samples, denoted by

$$\Delta d_{i,k}=v_{i,k}\cdot t_{i,k} \tag{8}$$

where $v_{i,k}$ denotes the kth speed value sampled from the ith KDE model, and $t_{i,k}$ the kth inter-arrival time is sampled from the exponential distribution, both corresponding to the ith trajectory tube.

Given the independence between speed and inter-arrival time, the PDF of the inter-aircraft distance is obtained via the convolution of their respective densities and yields

$$f_{\Delta Di}(\Delta d_i)=\lambda_i\int_0^{\infty}\frac{1}{t}f_{V_i}\left(\frac{d}{t}\right)\mathrm{e}^{-\lambda_i t}\mathrm{d}t \tag{9}$$

$$f_{\Delta Di}(\Delta d_i)=\int_{v_{\min}}^{v_{\max}}\frac{\lambda_i}{v_i}\mathrm{e}^{-\lambda_i\frac{\Delta d_i}{v_i}}f_{V_i}(v_i)\mathrm{d}v_i \tag{10}$$

where f_{V_i} is the speed PDF of the ith traffic flow; and $f_{\Delta Di}$ the PDF of the inter-aircraft distance in the ith traffic flow.

Fig. 5 illustrates the conceptual diagram of the inter-aircraft distance.

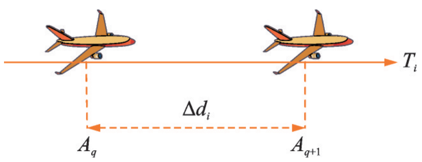

Fig.5 Inter-Aircraft distance

2.3.2 Remaining distance distribution

Traditional conflict risk assessments are typically based on static measures such as trajectory spacing or temporal separation. Although these metrics can reflect instantaneous states, they fail to capture the dynamic evolution characteristics of traffic flows. Trajectory spacing represents a static spatial snapshot that cannot describe the relative motion tendencies between aircraft, while temporal separation incorporates speed information but relies on specific assumptions (e.g., constant velocity) and lacks spatial intuitiveness in applications such as airspace planning and grid-based modeling.

To address these limitations, the concept of "remaining distance" is introduced. This concept originates from the idea of residual life in reliability engineering and renewal process theory, which describes the time interval from a random observation moment to the occurrence of the next event. Here, this time-domain concept is innovatively extended to the spatial domain to quantify, within the terminal area traffic flow, the spatial distance from any point in the airspace to the next aircraft arriving at that point.

Based on the inter-aircraft distance, the concept of remaining distance is defined as follows. For any aircraft A_q in the same flow, which represents the qth aircraft passing through a reference point P_0, its remaining distance is the distance between the projection of its current position onto the central trajectory and the reference point P_0. The remaining distance of the first aircraft is referred to as the first remaining distance. The PDF $f_{Ri}^q(r_i^q)$ of the remaining distance r_i^q for the qth aircraft can be derived from the PDF of the inter-aircraft distance $f_{\Delta Di}(\Delta d_i)$. For the first aircraft ($q=1$), the remaining distance r_i^1 is identical to the inter-aircraft distance d_i^1, so the PDF can be expressed as

$$f_{Ri}^1(r_i^1)=\frac{1}{\overline{\Delta d_i}}\left[1-F_{\Delta Di}(\Delta d_i^1)\right] \tag{11}$$

where $f_{Ri}^1(r_i^1)$ denotes the PDF r_i^1 of the remaining distance for the first aircraft approaching the reference point P in flow i. The function $F_{\Delta Di}$ represents the cumulative distribution function (CDF) of the inter-aircraft distance $f_{\Delta Di}$, obtained through numerical integration of the KDE results of the spacing distribution. The survival function $1-F_{\Delta Di}(\Delta d_i^1)$ quantifies the probability that the spacing exceeds the remaining distance, while $\overline{\Delta d_i}$ is the mean inter-aircraft distance in flow i, computed from Monte Carlo-sampled distance data. This mean is used for normalization, ensuring the PDF satisfies $\int_0^{\infty}f_{Ri}^1(r)\mathrm{d}r=1$.

When the number of aircraft is greater than two, the corresponding expression is given as

$$f_{Ri}^q=f_{Ri}^{q-1}*f_{\Delta Di}\quad q\geqslant 2 \tag{12}$$

where f_{Ri}^q denotes the probability of the remaining distance for the qth aircraft in flow i; and $*$ the convolution operator, indicating the superposition effect.

To further illustrate the concept of "remaining distance", a linear traffic flow F_i is considered in which all aircraft are assumed to maintain the same constant speed, and estimated by the maximum value of the speed distribution. Under the assumption that the arrival time distribution $f(\Delta t_i)$ follows an exponential distribution characterized by an arrival rate λ_i, the corresponding PDF $f_{\Delta Di}(\Delta d_i)$ is also exponential, characterized by the mean inter-aircraft distance $\overline{\Delta d_i}$.

$$f_{\Delta Di}(\Delta d_i)=\begin{cases}\dfrac{1}{\overline{\Delta d_i}}\mathrm{e}^{-\frac{1}{\overline{\Delta d_i}}\Delta d_i} & \Delta d_i \geqslant 0\\ 0 & \Delta d_i \leqslant 0\end{cases} \tag{13}$$

From Eq.(11), the probability function of the remaining distance for the first aircraft can be expressed as

$$f_{Ri}^1(r_i^1)=\begin{cases}\dfrac{1}{\overline{\Delta d_i}}\mathrm{e}^{-\frac{1}{\overline{\Delta d_i}}r_i^1} & r_i^1 \geqslant 0\\ 0 & r_i^1 \leqslant 0\end{cases} \tag{14}$$

Fig. 6 illustrates the conceptual diagram of the inter-aircraft remaining distance.

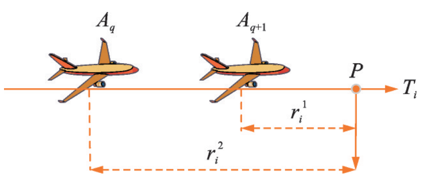

Fig.6 Inter-aircraft remaining distance

3 Potential Conflict Identification

Based on the structural characteristics of the terminal airspace, a 3D gridding approach is used to discretize the terminal area. By computing the intersection volume between each trajectory tube bounding box and the axis-aligned bounding box (AABB) centered at point P, together with PDFs of the traffic flow characteristics, the probability associated with each grid cell is obtained. These probabilities are then used to calculate the presence probability and potential conflict probability of each grid cell.

3.1 Gridding of terminal airspace

In terminal area operations, the standard horizontal separation is typically 6 km, and the vertical separation is 300 m. Therefore, the entire terminal airspace is discretized into a set of scatter points P arranged in a grid with dimensions of 6 000 m×6 000 m×300 m. Each point P serves as the center of a bounding box, which has the same dimensions of 6 000 m×6 000 m×300 m. For any grid point P, the nearest trajectory tube bounding box is determined using a nearest-neighbor search, and the local coordinate system of that bounding box is then used to generate the bounding box corresponding to point P. The global coordinates of point P are first transformed into the local coordinate system of the trajectory tube bounding box according to Eq.(15)

$$\boldsymbol{P}_{\mathrm{local}}=(\boldsymbol{P}_{\mathrm{global}}-\boldsymbol{C}_B)\cdot\boldsymbol{R}^{\mathrm{T}} \quad \boldsymbol{R}=[a,b,c] \tag{15}$$

where $\boldsymbol{P}_{\mathrm{local}}$ denotes the coordinates of point P in the local coordinate system; $\boldsymbol{C}_{\mathrm{B}}$ the center of the box, and $\boldsymbol{R}$ is the rotation matrix of the local coordinate system. $\boldsymbol{R}=[a, b, c]$ is the matrix composed of the axial vectors of the local coordinate system and used to describe its orientation and related directional information. Subsequently, an AABB centered at point P with dimensions of 6 000 m×6 000 m×300 m is generated.

To ensure that the geometric configuration of this bounding box aligns with the actual distribution of the traffic flow, rotation and translation operations are applied so that its orientation remains consistent with the flow direction of the trajectory tube. Specifically, using the rotation matrix $\boldsymbol{R}$ formed by the local coordinate axes and the center coordinate $\boldsymbol{C}_{\mathrm{B}}$ of the trajectory tube bounding box, the vertices of the bounding box in the local coordinate system are inversely transformed into the global coordinate system. In this way, a bounding box aligned with the trajectory tube's flow direction is obtained. This bounding box is subsequently used to calculate the intersection volume between itself and the trajectory tube bounding box.

3.2 Intersection volume between trajectory tube and AABB

The intersection volume between the AABB centered at point P and all trajectory tube bounding boxes is computed using the AABB algorithm. Based on the separating axis theorem (SAT), the algorithm is optimized for AABBs by analyzing the projection intervals of the two boxes along the three coordinate axes to determine whether an intersection exists.

As illustrated in Fig.7, the overlapping region between the two cuboids represents the intersection volume of the trajectory tube bounding box and the AABB centered at point P. Each box is projected onto the three coordinate axes of the global coordinate system to obtain their respective projection intervals. The maximum and minimum coordinates of both boxes are then calculated in the global coordinate frame to determine the overlapping range. Based on this range, the intersection volume between the trajectory tube bounding box and the AABB is computed.

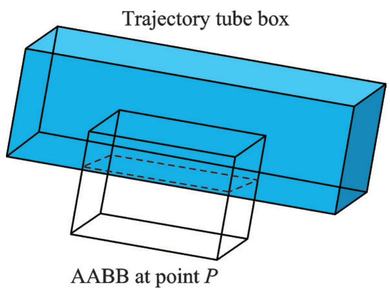

Fig.7 Definition of the intersection volume

After determining the intersection volume, points P with non-zero intersection volumes are selected. These points are subsequently used to calculate the presence probability and potential conflict probability in the vicinity of point P.

3.3 Presence probability

The presence probability map is constructed based on 15 min time windows and reflects the probability that at least one aircraft is present in the vicinity of point P, i.e., within the bounding box centered at P, during a given time interval. In other words, it represents the probability that an aircraft exists near point P.

For any point P, a single trajectory tube bounding box B_i^k is considered, where B_i^k corresponds to the kth box of flow i. Let $P_1(P, B_i^k)$ denote the probability that an aircraft exists near point P (within the range of box B_i^k), that is, the probability that at least one aircraft is located inside the bounding box of point P. Since the aircraft distributions in the lateral, the longitudinal, and the vertical directions are mutually independent, the presence probability can be expressed as

$$\begin{aligned} P_1(P,B_i^k) &= P(\exists A_{Ci}\in P_i^k(P))= \\ & P(\exists A_{Ci}\in[\overline{A},\underline{A}])\cdot P(\exists A_{Ci}\in[\overline{B},\underline{B}])\cdot \\ & P(\exists A_{Ci}\in[\overline{C},\underline{C}]) \end{aligned} \tag{16}$$

where $P(\exists A_{Ci}\in P_i^k(P))$ denotes the probability that an aircraft A_{Ci} is located within the bounding box $P_i^k(P)$ centered at point P. The term $P(\exists A_{Ci}\in[\overline{A}, \underline{A}])$ represents the probability that an aircraft exists within the interval $[\overline{A}, \underline{A}]$ along the A-direction of the A_{C_i} coordinate system, that is, along the lateral axis; $P(\exists A_{Ci}\in[\overline{B}, \underline{B}])$ the probability of aircraft presence within the longitudinal interval $[\overline{B}, \underline{B}]$; and $P(\exists A_{Ci}\in[\overline{C}, \underline{C}])$ the probability of aircraft presence within the vertical interval $[\overline{C}, \underline{C}]$.

Based on the results of the intersection volume calculation, the intersection boundaries between each point P and the trajectory tube bounding boxes are determined. For each box B_i^k of flow F_i, the local intersection boundary with point P is obtained, which defines the effective presence region of aircraft in the lateral, the longitudinal, and the vertical directions.

Subsequently, the probabilities along the three directions are determined respectively.

$$P(\exists A_{Ci}\in[\overline{A},\underline{A}])=\int_{\underline{A}}^{\overline{A}} f_{ai}^k/\underline{A}(x)\mathrm{d}x \tag{17}$$

$$P(\exists A_{Ci}\in[\overline{B},\underline{B}])=\int_0^{\underline{B}\overline{B}} f_{Ri}^1(y)\mathrm{d}y \tag{18}$$

$$P(\exists A_{Ci}\in[\overline{C},\underline{C}])=\int_{\underline{C}}^{\overline{C}} f_{ci}^k/\underline{C}(z)\mathrm{d}z \tag{19}$$

The upper and the lower bounds in the lateral and the vertical directions are determined by the intersection range in the local coordinate system, and their integrands are computed using CDF of the normal distribution. In the longitudinal direction, the lower bound is set to zero, while the upper bound corresponds to the maximum intersection range along that direction in the local coordinate system. The integrand in this case is obtained through the analytical integration of the remaining distance PDF.

Subsequently, the probability is extended to the entire trajectory tube, representing the probability that at least one bounding box within a single flow F_i contains an aircraft. This probability is calculated using the complementary probability method and expressed as

$$P_{F_i}=1-\prod_{K=1}^{K}(1-P_1(P,B_i^k)) \tag{20}$$

Finally, the probability is extended to all trajectory tubes, representing the probability that at least one aircraft exists in the vicinity of point P, which can be expressed as

$$P_1(P)=1-\prod_{i=1}^{N}(1-P_{F_i}) \tag{21}$$

3.4 Potential conflict probability

The potential conflict probability map is constructed based on 15 min time windows to represent the probability that at least two aircraft from different traffic flows are simultaneously present in the vicinity of point P, i.e., within the bounding box centered at P, during a given time interval.

The potential conflict probability at point P is expressed as

$$P_2(P)=P_1(P)-\sum_{i=1}^{N}P_1(P,F_i)\prod_{j=1,j\neq i}^{N}(1-P_1(P,F_j)) \tag{22}$$

where $P_1(P,F_i)\prod_{j=1,j\neq i}^{N}(1-P_1(P,F_j))$ represents the probability that only flow F_i exists at point P, while all other flows do not exist. $P_1(P,F_i)$ represents the probability that at least one aircraft in flow F_i is near point P. $\prod_{j=1,j\neq i}^{N}(1-P_1(P,F_j))$ represents the probability that no aircraft exists in any flow other than flow F_i. The single flow is extended to all flows within the terminal area, $\sum_{i=1}^{N}P_1(P,F_i)\prod_{j=1,j\neq i}^{N}(1-P_1(P,F_j))$ is the total probability that exactly one flow has an aircraft near point P, the sum of the probabilities that only the i-th flow exists while all other flows do not exist, and the final $P_2(P)$ is the probability that at least two flows exist near point P.

4 Case Analysis

In this study, 3D presence probability maps and potential conflict probability maps are constructed to achieve a visualized representation of terminal airspace situations. Points P at the same altitude are extracted to generate two-dimensional hotspot maps for different flight levels, enabling the identification of potential conflict regions and the corresponding interacting traffic flows responsible for these conflicts.

4.1 Presence probability map

Following the point selection method described in Section 3, scatter points P are distributed throughout the entire terminal airspace at intervals of 6 000 m×6 000 m×300 m, and a bounding box centered at each point P is generated. Fig.8 shows the 3D presence probability map for regions with probabilities greater than zero. As shown in Fig.8, the 3D trajectories of aircraft belonging to different traffic flows can be clearly observed, extending from the terminal entry points to the landing phase. Fig.9 illustrates the presence probability maps at different flight levels. In Figs.9(a—i), the sequential progression of aircraft during the approach phase, from the terminal entry points to the final approach and landing, can be clearly observed.

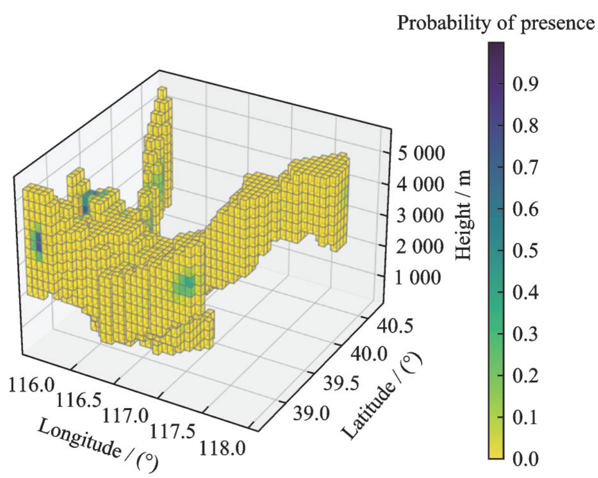

Fig.8 3D presence probability map

4.2 Potential conflict probability map

Fig.10 shows the 3D potential conflict probability map formed by points with probabilities greater than zero. Fig.11 depicts the potential conflict probability maps at different flight levels. Based on the latitude and the longitude data, the regions where potential conflicts are most likely to occur at each flight level can be identified.

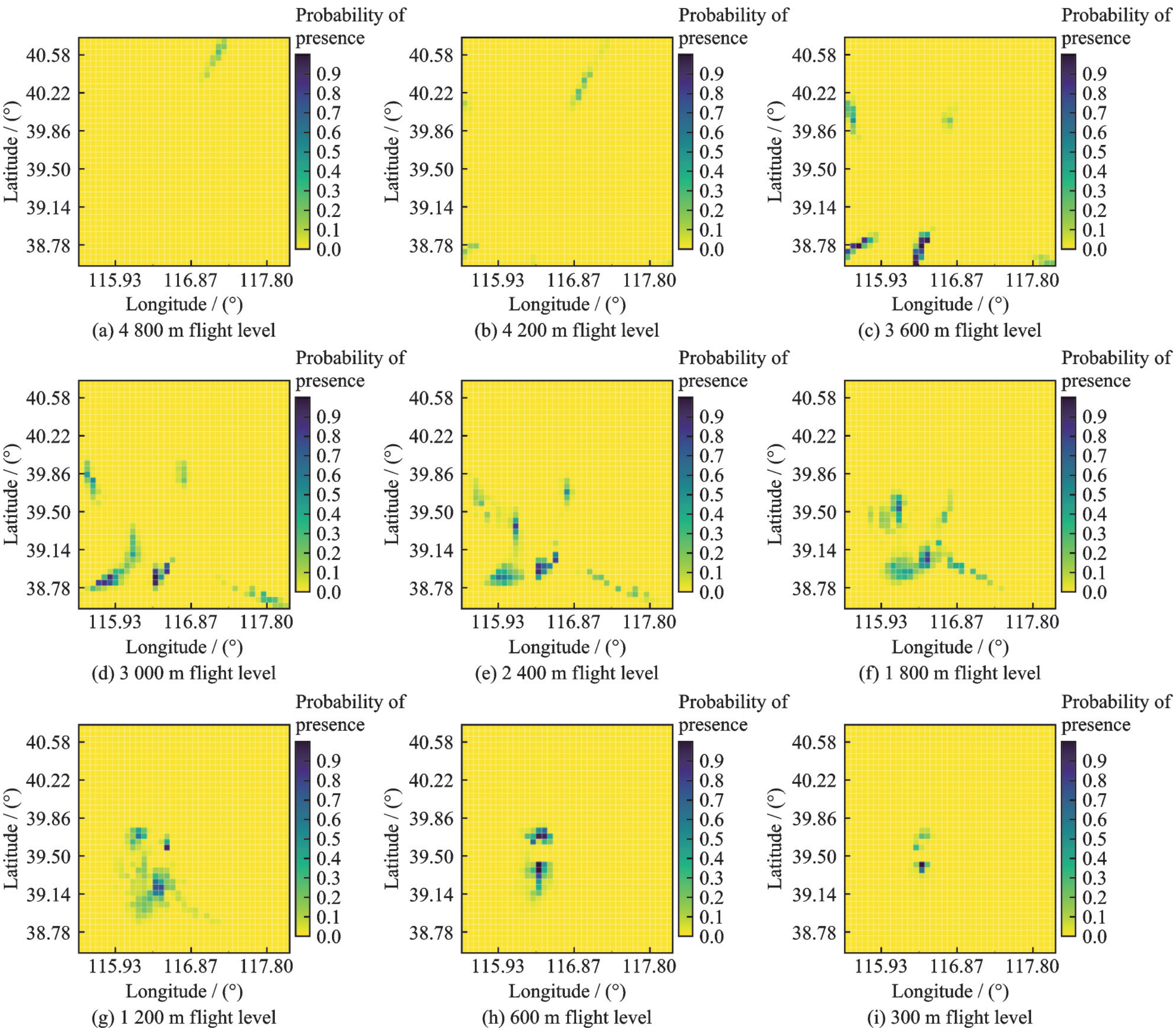

Fig.9 Presence probability maps at different flight levels

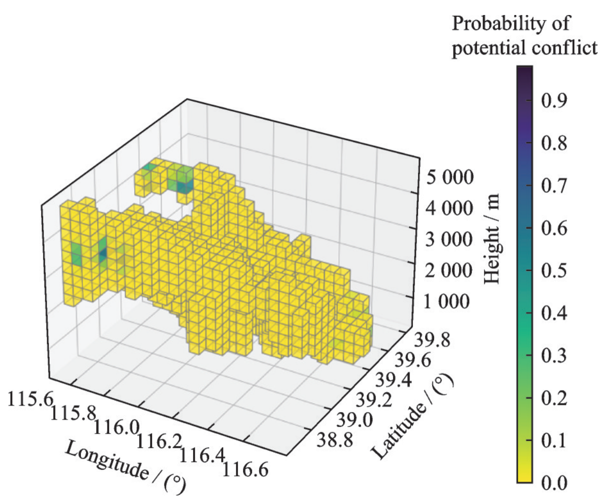

Fig.10 3D potential conflict probability map

Fig. 12 illustrates the traffic flows that contribute to potential conflicts at different flight levels. The numbers within each grid cell represent the identifiers of traffic flows involved in potential conflicts, revealing the interaction mechanisms of conflicting flows across various flight levels. The analytical results show a high degree of consistency with actual terminal-area air traffic control operations, thereby verifying the effectiveness of the proposed method.

Specifically, when aircraft come from the same terminal entry point, the potential conflict probability is significantly reduced at lower flight levels. This reduction occurs because controllers typically complete sequencing and spacing adjustments during the approach phase. For example, traffic flows 4 and 5, which originate from the same entry point, exhibit potential conflicts primarily concentrated between 3 600 m and 2 400 m. Within this flight level range, an average of approximately six conflict points are observed per level, while no conflicts are detected

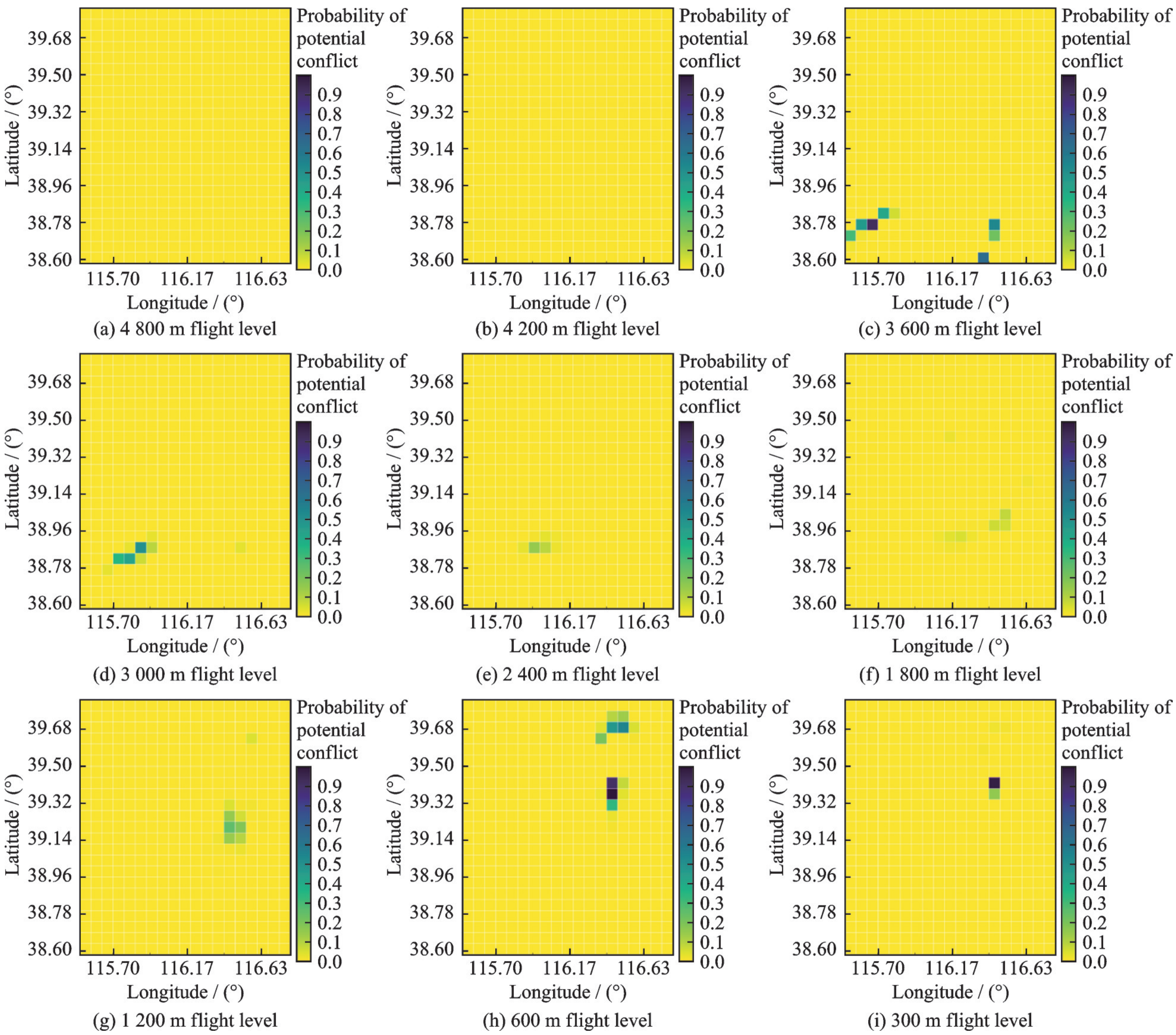

Fig.11 Potential conflict probability maps at different flight levels

below 2 100 m, indicating that low flight level conflict risks have been effectively mitigated.

In contrast, for traffic flows coming from different terminal entry points, such as flows 1 and 3, the initial trajectories intersect at large angles, and the coordination process involves multiple control sectors and complex procedures. Consequently, no significant conflicts are observed at higher flight levels (3 600—2 700 m), while conflict points are mainly concentrated below 1 800 m. Notably, at 900 m, the number of conflict points reaches 20, while at 1 200 m and 600 m, the counts reach 15 and 13, respectively. This distribution indicates a significant increase in conflict risk during the final approach and landing phases. The observed pattern aligns well with the actual operational characteristics of terminal airspace: Aircraft from different entry points generally maintain independent operation at higher flight levels, whereas at lower flight levels where flight paths converge and airspace resources become constrained the risk of conflict increases markedly, requiring controllers to resolve potential conflicts dynamically through real-time instructions.

These quantitative findings not only confirm the capability of the proposed method to identify mid-term potential conflict risks within the terminal area but also clearly reveal the evolutionary pattern of risk hotspots through the spatial density of conflict points. The results provide practical decision-support value for air traffic controllers. For instance, at low flight level regions where flows from different entry points converge, optimized approach route designs or traffic flow management strategies can be developed in advance based on the number of

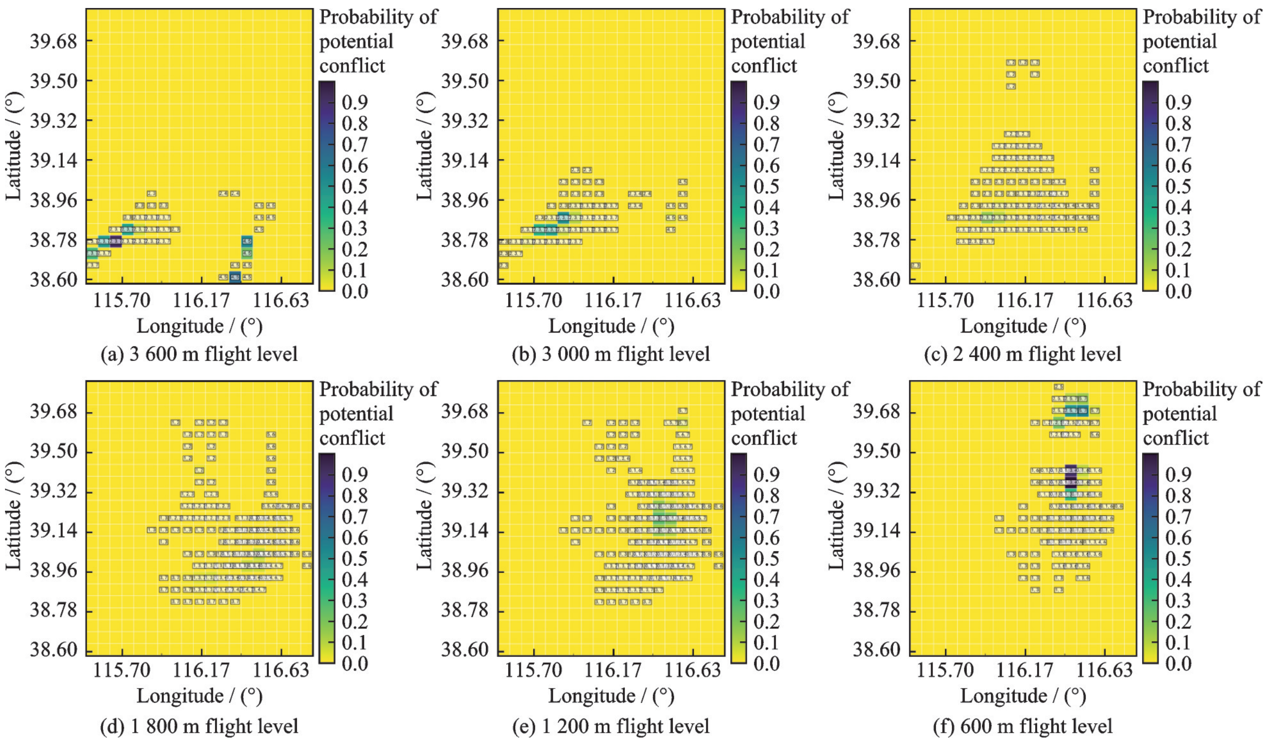

Fig.12 Potential conflicting traffic flows at different flight levels

detected conflict points, thereby enhancing both the safety and operational efficiency of terminal airspace management.

4.3 Results analysis

To validate the feasibility of the constructed potential conflict identification method in actual operational environments, this paper introduces a practical verification approach independent of the potential conflict identification model based on flight trajectory data. Using whether aircraft experienced safety separation violations during real operations as the criterion, the method directly analyzes instantaneous flight trajectory data to identify aircraft pairs potentially facing actual conflict risks. It then compares the consistency between the model's identification results and actual operational characteristics. First, the horizontal separation, the vertical separation, and the duration of separation between aircraft pairs within the same time interval are calculated to screen out pairs exhibiting insufficient separation during operations. When two aircraft have a horizontal separation less than 6 km, a vertical separation less than 300 m, and the separation remains inadequate for 10 s, they are classified as a potential conflict pair. Subsequently, the identified potential conflict pairs are compared with the potential conflict zones detected by the model. This dual verification approach examines whether the aircraft pair spatially overlaps with the conflict zone identified by the model and analyzes whether their associated traffic flow combination aligns with the high-risk traffic flow interweaving patterns detected by the model. This method enables systematic validation of potential conflict identification results from both spatial positioning and traffic flow structure perspectives.

One potential conflict aircraft pair identified by this method is shown in Fig.13, depicting its terminal approach trajectory, while Fig.14 illustrates the altitude changes of both aircraft. Figs.13, 14 reveal the latitude, the longitude, and the altitude where the potential conflict occurs. CZ3165 (3.25) belongs to traffic flow 3, while JD5252 (3.25) belongs to traffic flow 4. The altitude chart indicates that JD5252 (3.25) performs a go-around maneuver.

Analysis of the altitude chart indicates that the primary potential conflict zone is concentrated between 300 m and 600 m. Therefore, the two-dimensional flight trajectories of the potential conflict aircraft pairs are compared with the potential conflict probability map identified in this chapter to analyze whether they occur in the same zone and whether

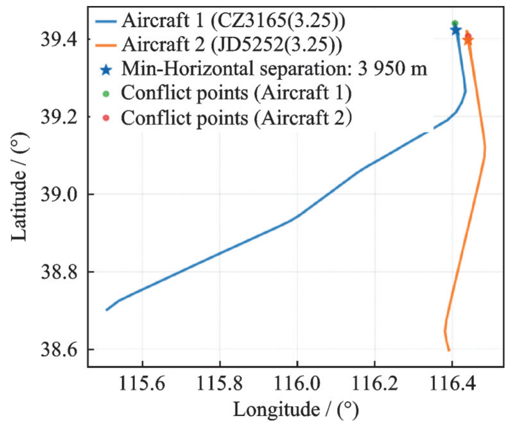

Fig.13 Latitude-longitude trajectories of potential conflict aircraft pairs

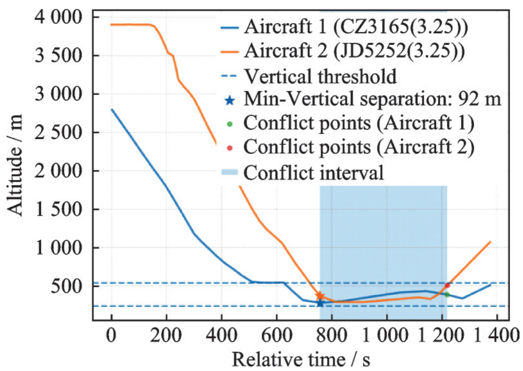

Fig.14 Altitude profiles of potential conflict aircraft pairs

the traffic flows match. Figs.15, 16 show the comparison maps for the 600 m and 300 m flight levels, respectively.

Figs.15, 16 show that the potential conflict aircraft perfectly align with the corresponding potential conflict zones identified by the model. Both aircraft belong to traffic flows 3 and 4, corresponding to the 300 m and 600 m potential conflict zones. The traf-

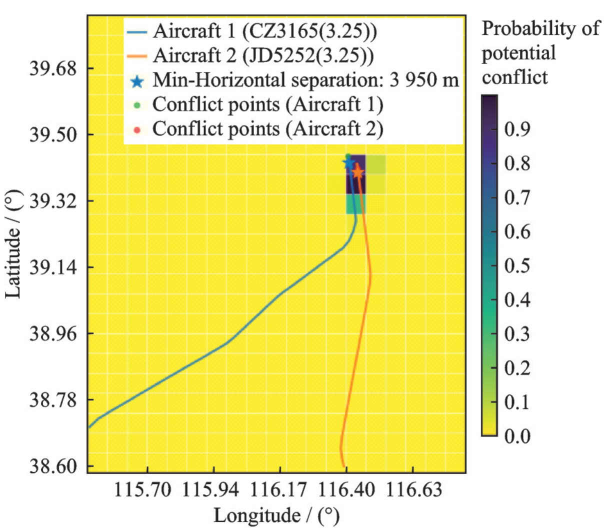

Fig.15 600 m flight level comparison chart

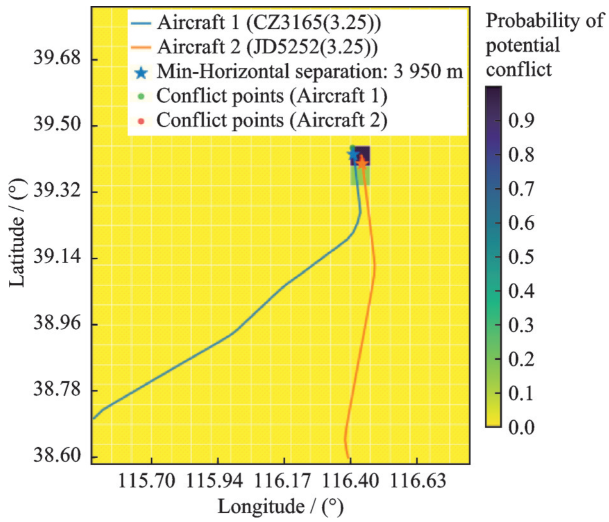

Fig.16 300 m flight level comparison chart

fic flows generating potential conflicts in this area are 0, 1, 3, 4, and 6, including flows 3 and 4. This validates the effectiveness and accuracy of the method.

5 Conclusions

This study proposes a data-driven method for 3D traffic flow generation. Based on this method, a probabilistic modeling framework is used to identify and characterize potential conflict regions within terminal airspace. Using a representative terminal area as a case study, the approach effectively identifies potential arrival conflict regions. The main conclusions are drawn as follows.

(1) A 3D trajectory tube model is developed on the basis of two-dimensional clustering, enabling the construction of a 3D traffic flow model that effectively captures the spatial distribution characteristics of flight trajectories and provides a solid 3D data foundation for conflict identification.

(2) The concept of remaining distance is introduced to characterize aircraft-following behavior. By analyzing the distribution of remaining distance, potential chase or convergence situations between aircraft can be identified. The potential conflict region identification model detects potential conflict zones across different flight levels within the same time window, quantifies the probability of potential conflicts, and determines the interacting traffic flows responsible for these conflicts, thereby revealing the inter-flow influence relationships.

(3) The terminal airspace is discretized through a 3D gridding process, enabling spatial partitioning and precise localization of potential conflict hotspots. This approach narrows the spatial scope of conflict identification from the macroscopic airspace level to specific grid cells, significantly enhancing spatial resolution and providing a more accurate spatial reference for conflict warning and regulation.

(4) The effectiveness of the proposed method is validated. By identifying potential conflict regions and analyzing the interactions among traffic flows, the method provides valuable decision-support capability for traffic flow planning in flow management, controller decision assistance, and airspace design and analysis, ultimately contributing to improved safety and operational efficiency in terminal area management.

Future work will focus on incorporating dynamic meteorological factors, such as wind fields, turbulence, and visibility constraints, into the probabilistic conflict identification framework. By integrating real-time weather data into the trajectory tube model, the influence of environmental uncertainties on aircraft position and speed distributions can be quantified, further enhancing the method's adaptability and robustness in complex terminal operations.

References

[1] ZHANG Feiqiao, ZHANG Yichi, YAN Hao. Improved convolutional network based 4D trajectory prediction and conflict detection in terminal areas[J]. Science Technology and Engineering, 2024, 24(5): 2150-2157. (in Chinese)

[2] MATSUNO Y, TSUCHIYA T, WEI J, et al. Stochastic optimal control for aircraft conflict resolution under wind uncertainty[J]. Aerospace Science and Technology, 2015, 43: 77-88.

[3] DUDOIT A, RIMŠA V, BOGDEVIČIUS M. Investigation of aircraft conflict resolution trajectories under uncertainties[J]. Sensors, 2024, 24(18): s2418.

[4] YANG Z J, KANG X L, GONG Y H, et al. Aircraft trajectory prediction and aviation safety in ADS-B failure conditions based on neural network[J]. Scientific Reports, 2023, 13: 19677.

[5] XU Q C, CHEN Z Q, LI F F, et al. An efficient aircraft conflict detection and resolution method based on an improved reinforcement learning framework[J]. International Journal of Aerospace Engineering, 2023: 6643903.

[6] ZHANG W. A data-driven methodology for aircraft trajectory analysis to improve mid-air conflict detection in terminal airspace[D]. Atlanta, USA: Georgia Institute of Technology, 2024.

[7] BAO J, ZHANG Z J, ZHANG J F, et al. Exploring the conflict risk characteristics of air weaving sections in Metroplex terminal areas with flight trajectory data and adaptive graph spatial-temporal transformer[J]. Journal of Air Transport Management, 2024, 120: 102667.

[8] WANG Xinglong, ZHOU Duyi. Identification of critical grid areas in flight area conflicts based on complex network[J]. Journal of Safety Science and Technology, 2023, 19(8): 32-38. (in Chinese)

[9] SHVETSOV A V. Analysis of accidents resulting from the interaction of air and ground vehicles at airports[J]. Transportation Research Procedia, 2021, 59: 21-28.

[10] WANG Hongyong, MA Lishu. Assessment and evolution analysis of traffic complexity in terminal area[J]. Science Technology and Engineering, 2024, 24(21): 9235-9243. (in Chinese)

[11] WANG Hongyong, GUO Yupeng. Air traffic complexity model based on aircraft self-separation operation[J]. Journal of Transportation Systems Engineering and Information Technology, 2022, 22(2): 305-312, 321. (in Chinese)

[12] WU Minggong, WANG Zekun, GAN Xusheng, et al. Identification of key flight conflict nodes based on complex network theory[J]. Journal of Northwestern Polytechnical University, 2020, 38(2): 279-287. (in Chinese)

[13] GARCÍA-OVIES CARRO I, ARNALDO VALDÉS R M. Analysing sector safety performance based on potential conflicts: Complex network approach[J]. Aerospace, 2024, 11(11): 0891.

[14] WANG C, HAN B C, LIU F. Analysis on potential conflict frequency of intersected air routes in terminal airspace design[J]. Transactions of Nanjing University of Aeronautics and Astronautics, 2014, 31(5): 580-588.

[15] FIGUET B, MONSTEIN R, WALTERT M, et al. Data-driven mid-air collision risk modelling using extreme-value theory[J]. Aerospace Science and Technology, 2023, 142: 108646.

[16] HU Z Y, GAN X S, WU Y R, et al. Research on conflict detection in terminal area based on Monte Carlo method[C]//Proceedings of 2022 IEEE International Conference on Advances in Electrical Engineering and Computer Applications (AEECA). Dalian, China: IEEE, 2022: 455-459.

[17] LI Y Y, TIAN Y, XIE X X, et al. Bayesian spatio-temporal trajectory prediction and conflict alerting in terminal area[J]. Aerospace, 2025, 12(9): 12090855.

[18] HAO Siqi. Research on aircraft conflict detection and resolution under four-dimensional trajectory-based operation[D]. Harbin, China: Harbin Institute of Technology, 2020. (in Chinese)

[19] LIU R W, HAO S Q, ZHANG Y P, et al. A novel strategic aircraft track planning method considering conflict probability[J]. Aerospace, 2022, 9(12): 9120848.

[20] LIU Z Q, NAN Y, YANG Y. Airspace conflict detection method based on subdivision grid[C]//Proceedings of Artificial Intelligence in China. Singapore: Springer Singapore, 2022: 670-677.

[21] ZHU Yongwen, XIE Hua, PU Fan, et al. Research of airspace gridding method and its application in air traffic management[J]. Advances in Aeronautical Science and Engineering, 2021, 12(4): 12-24. (in Chinese)

[22] ZHOU Y, HU M H, YANG L, et al. Collaborative conflict-free 4D trajectory planning based on multi-objective hybrid-metaheuristic optimization algorithm[J]. Transactions of Nanjing University of Aeronautics and Astronautics, 2024, 41(3): 372-386.

Acknowledgements This work was supported in part by the National Natural Science Foundation of China (Nos. U2333204, U1833103).

Author

The first/corresponding author Ms. **LI Nan** received her B. S. degree in computer science and application from Department of Computer Science &Technology from Civil Aviation University of China, Tianjin, China, in 2000 and M. S. degree in navigation guidance and control from College of Air Traffic Management, Civil Aviation University of China in 2003. She is currently an associate professor and master's degree tutor in College of Air Traffic Management, Civil Aviation University of China. Her research focuses on transportation planning and management, and air traffic control simulation verification.

Author contributions Ms. **LI Nan** designed the study, provided the cases and idea, conducted the analysis. Mr. **LIU Xinrui** complied the models and wrote the manuscript. Mr. **PENG Jiayi** contributed to the data collection and data analysis. Mr. **ZHU Yan** analyzed the experimental results in comparison with actual terminal-area air traffic control operations and secured the funding for the project associated with this publication. Prof. **WANG Hongyong** contributed to the discussion and background of the study. All authors commented on the manuscript draft and approved the submission.

Competing interests The authors declare no competing interests.

(Production Editor: ZHANG Bei)

基于三维轨迹管的终端区交通流潜在冲突识别

李 楠[1], 刘昕瑞[1], 彭佳懿[2], 朱 棪[3], 王红勇[1]

(1.中国民航大学空中交通管理学院,天津 300300,中国; 2.中国民用航空空中交通管理局空域中心,北京 101300,中国; 3.中国民用航空新疆空中交通管理局,乌鲁木齐 519015,中国)

摘要:针对终端空域交通运行密度大幅提升、航空器间潜在冲突加剧的问题,本文提出一种基于三维(Three-dimensional, 3D)航迹管结构的终端空域潜在冲突识别方法,旨在为终端空域运行安全与效率提升提供完善的理论分析框架。该方法首先对进场航迹开展聚类分析,提取主流交通流并构建对应的三维轨迹管;随后将交通流特征参数引入概率模型,并结合三维空域网格分析,实现潜在冲突区域的识别与定位。实验结果表明,所提方法能够在15 min时间窗口内有效识别潜在冲突区域,并可量化分析区域内各交通流之间的相互干扰关系。本研究构建的理论分析框架对空域优化设计、辅助管制决策兼具理论价值与工程实用意义,可为提升终端空域运行安全与运行效率提供参考。

关键词:终端区;交通流;潜在冲突识别;核密度估计;轨迹管

研究亮点:

1.构建三维轨迹管表征方法,实现终端区进场交通流的结构化三维建模,突破传统二维航迹分析的维度局限,可量化描述交通流的三维空间分布与概率密度特征。

2.构建三维网格化概率冲突识别模型,可精准定位空域冲突热点区域及对应交通流组合,实现由微观单机冲突检测向宏观交通流冲突分析转变。